

## GRID CONNECTED SOLAR PV SYSTEM OF THREE PHASE MULTILEVEL INVERTER WITH SINUSOIDAL PULSE WIDTH MODULATION TECHNIQUE

<sup>1</sup> A. Mahesh Kumar, <sup>2</sup>Komati Chandra Shaker

<sup>1</sup> Dept of EEE, Mahaveer Institute of Science & Technology College, Hyderabad, TS, India

<sup>2</sup> Dept of EEE, Avanti Institute of Engineering and Technology, Hyderabad, TS, India

**Abstract:** The Solar Photovoltaic (SPV) systems which directly supply power to the grid are becoming more widely used. The photovoltaic (PV) field has given rise to a global industry capable of producing many gig watts (GW). The active and reactive power feed-in by grid-connected solar PV systems will result in voltage rise over its maximum limit in distribution systems. In This Project proposes different voltage control strategies to limit the voltage rise in low voltage distribution systems caused by grid connected solar PV systems. The voltage control strategies include four different active and reactive power control strategies. A power electronic converter which converts DC power from the PV array to AC power at required voltage and frequency levels is known as Inverter. Generally different Pulse Width Modulation (PWM) techniques have been implemented for grid connected 3-phase Voltage Source Inverter (VSI) system. On the basis of discussion of harmonic injection SPWM (HI-SPWM) and voltage space vector PWM (VSV-PWM), a Sinusoidal PWM technique (SPWM), which is really simplest and well designed to obtain maximum inverter gain, minimum switching frequency and to avoid the disadvantages of HI-SPWM, is proposed. The SPWM is based on instantaneously floating the equivalent neutral point of the output of a 3-phase inverter i.e. instantaneously injecting the same voltage waveform into the phase voltages. Modeling of photovoltaic systems includes modeling of SPV array, power electronics inverter/converter based on MATLAB/SIMULINK.

**Keywords:** Photovoltaic Array, Sinusoidal Pulse width modulation, three phase voltage source inverter, LC filter.

### I. Introduction

In the present scenario of world energy sector renewable sources are growing their importance day by day. This is mainly because of limited resource and bad environmental impacts of the conventional energy. Having realized the importance of finding alternative energy resources for the future energy sustainability, photovoltaic (PV) energy has become one of the important renewable energy sources [1]. Photovoltaic (often abbreviated as PV) are a simple and elegant method of harnessing the sun's energy. PV devices (solar cells) are unique in that they directly convert the incident solar radiation into electricity, with no noise, pollution or moving parts, making them robust, reliable and long lasting. The output of solar PV arrays is dependent on the level of solar irradiance and surface temperature of the array itself. Maximum power output from the array can be achieved by a combination of mechanical solar trackers to maximize the amount of light received, and a maximum power point tracking (MPPT) algorithm to operate the PV array around its maximum power output for a given load under varying atmospheric conditions. With the aid of electronics power converters mainly the dc (direct current) boost converters and inverters, this kind of energy can be utilized and transported to the electric utility [2]-[4]. However, the inverter efficiency need to be improved further on in order to mitigate the effects of the self-consumption losses, unbalanced load on inverter output voltage, nonlinearity, PV low

efficiency and output fluctuation [5], electromagnetic interference and high level of harmonics content [6]. In addition, it is important that the inverter system acquires the capability to operate with high speed and frequency in generating the pulse-width modulation (PWM) signals. Hence, the inverter controller which plays an important role in the improvement of the abovementioned issues, needs to be enhanced further to uplift the inverter performance in renewable energy applications, especially in PV.

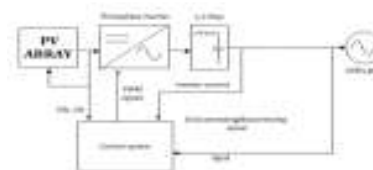


Fig.1. Block diagram of the grid-connected inverter PV system

### II. Grid Connected Solar Pvsystem

The general grid connected SPV system is shown in Fig.1 First stage PV array or module is connected with the system which connects the input to the inverter. The 3-phase VSI is used to convert DC voltage to AC voltage and feeds the energy to the load and grid [11] through LC filter circuit. The inverter has to be controlled in order to obtain harmonic less voltage to achieve good power quality. Various PWM techniques are used to switch the inverter circuit. A PLL is used for proper synchronization

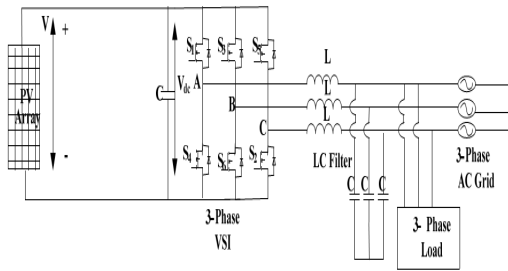


Fig.2 General Block Diagram of Grid Connected SPV system

**A. Modeling of Solar PV**

A solar cell is basically a p-n junction fabricated in a thin wafer of semiconductor. The electromagnetic radiation of solar energy can be directly converted to electricity through Photovoltaic effect. Being exposed to the sunlight, photons with energy greater than the band-gap energy of the semiconductor creates some electron-hole pairs proportional to the incident irradiation. The output voltage of the solar cell is a function of the photocurrent that depends on the solar irradiation level during its operation [7]-[10].

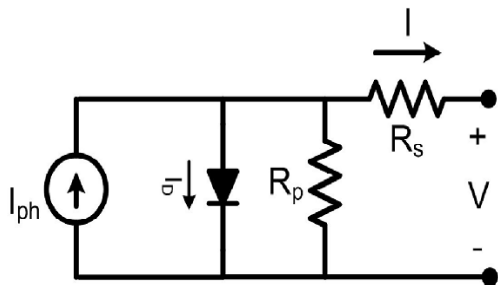


Fig.3 Simplified PV cell model

A model of PV module with moderate complexity that includes the temperature independence of the photocurrent source, the saturation current of the diode, and a series Resistance is considered based on the Shockley diode equation. The current source  $I_{ph}$  represents the cell photocurrent.  $R_{sh}$  and  $R_s$  are the intrinsic shunt and series resistances of the cell, respectively. Usually the value of  $R_{sh}$  is very large and that of  $R_s$  is very small, hence they may be neglected to simplify the analysis. PV cells are grouped in larger units called PV modules which are further interconnected in a parallel-series configuration to form PV arrays. The current output of PV module is

$$I_{pv} = N_p * I_{ph} - N_p * I_0 \left[ \exp\left(\frac{q * (V_{pv} + I_{pv} R_s)}{N_s A k T}\right) - 1 \right] \quad (1)$$

Where  $I_{pv}$  is the PV array output current,  $V_{pv}$  is the PV array output voltage,  $I_{ph}$  is module photo current,  $R_s$  is the series resistance,  $k$  is the Boltzmann constant ( $1.38 \times 10^{-23}$  J/K),  $A$  is the ideal factor,  $N_s$  is the series no of cells and  $N_p$  is parallel number of cells.  $T$  is the operating temperature [11].

Below are the specifications of the PV module:

- (i) Open circuit output voltage,  $V_{oc} = 30.6$  V
- (ii) Short circuit output current,  $I_{sc} = 8.5$  A
- (iii) Maximum power output voltage,  $V_{mp} = 24.3$  V
- (iv) Maximum power output current,  $I_{mp} = 7.8$  A

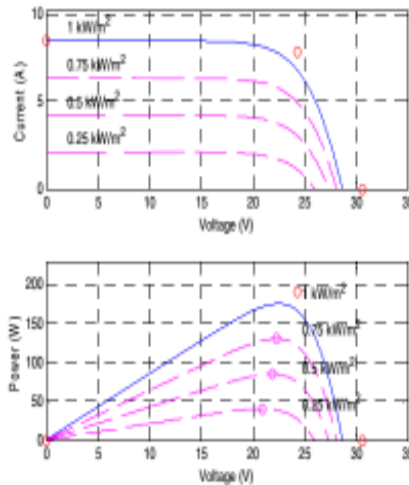


Fig.3 I-V and P-V characteristics of a one PV module

**B. Three Phase Voltage Source Inverter**

A 3-phase VSI is used to convert DC voltage into AC voltage and feeds power to consumer loads and utility grid. The 3-phase inverters are used in grid connected SPV systems. A 3-phase inverter is a six step bridge inverter. It uses a minimum of six devices. As stated earlier, the transistor family of devices is now very widely used in inverter circuits. Presently the use of IGBT in three-phase inverter is on the rise. A capacitor connected at the input terminals tends to make the input dc voltage constant. This capacitor also suppresses the harmonics fed back to the source. In inverter terminology, a step is defined as a change in the firing from one IGBT to the next IGBT in proper sequence. For one cycle of 360, each step would be of 60 intervals for a six step inverter. This means that the IGBT would be gated at regular intervals of a six step inverter. There are two possible patterns of gating the switches. In one pattern, each switch conducts for 180 and in the other each switches conducts for 120. But in both these patterns gating signals are applied and removed at 60 intervals of the output voltage [12]. A LC type filter is used to provide 50Hz frequency output to consumer loads and electric grid. There are various factors which decide the selection of filter capacitor and inductor. Generally in order to eliminate the higher order harmonics, the resonant frequency of the filter should be greater than 6 times of desired output frequency [13].

**III. Mathematical Model Of Lc Filter**

The mathematical model of LC filter circuit has been derived using state space analysis [14]. LC output filter circuit for voltage and current equations is shown in Fig.4. Kirchoff’s current law is applied to the nodes a, b, c shown in Fig.4.

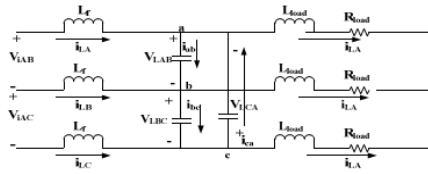


Fig.4. LC Filter Circuit

At node a,

$$i_{iA} + i_{ca} = i_{ab} + i_{LA} \Rightarrow i_{iA} + C_f \frac{dV_{LCA}}{dt} = C_f \frac{dV_{LBC}}{dt} + i_{LB} \quad (2)$$

At node b,

$$i_{iB} + i_{ab} = i_{bc} + i_{LB} \Rightarrow i_{iB} + C_f \frac{dV_{LAB}}{dt} = C_f \frac{dV_{LBC}}{dt} + i_{LB} \quad (3)$$

At node c,

$$i_{iC} + i_{bc} = i_{ca} + i_{LC} \Rightarrow i_{iC} + C_f \frac{dV_{LBC}}{dt} = C_f \frac{dV_{LCA}}{dt} + i_{LC} \quad (4)$$

To make state equations, Kirchoff’s voltage law is applied to inverter side and load side and finally state space equation for LC filter circuit is given in (5).

$$\dot{X}(t) = AX(t) + Bu(t) \quad (5)$$

$$X = \begin{bmatrix} V_L \\ I_i \\ I_L \end{bmatrix}_{9 \times 1}, \quad A = \begin{bmatrix} 0_{3 \times 3} & \frac{1}{3C_f} I_{3 \times 3} & \frac{-1}{3C_f} I_{3 \times 3} \\ \frac{-1}{L_f} I_{3 \times 3} & 0_{3 \times 3} & 0_{3 \times 3} \\ \frac{1}{L_{load}} I_{3 \times 3} & 0_{3 \times 3} & \frac{-R_{load}}{L_{load}} I_{3 \times 3} \end{bmatrix}_{9 \times 9}$$

$$B = \begin{bmatrix} 0_{3 \times 3} \\ \frac{1}{L_f} I_{3 \times 3} \\ 0_{3 \times 3} \end{bmatrix}_{9 \times 3}, \quad u = [V_i]_{3 \times 1}$$

Where  $V_L = [V_{LAB} \ V_{LBC} \ V_{LCA}]^T$ ,  $I_i = [i_{iAB} \ i_{iBC} \ i_{iCA}]^T$ ,  $V_i = [V_{iAB} \ V_{iBC} \ V_{iCA}]^T$ ,  $I_L = [i_{LAB} \ i_{LBC} \ i_{LCA}]^T$

(6)

**PWM TECHNIQUES FOR 3-PHASE VSI**

This section describes two types of PWM techniques used to control the 3-phase VSI of a grid connected SPV system.

**Sinusoidal PWM (SPWM)**

The SPWM technique is very simple and very easy to implement. This method produces a sinusoidal waveform by filtering an output pulse waveform by varying width. The required output voltage is achieved by varying the amplitude and frequency of modulating voltage. The pulse width can be changed by changing the amplitude and frequency of

reference or modulating voltage. In Fig.5, modulating wave is compared with high frequency triangular wave from. The high switching frequency leads better output sinusoidal wave from. The switching state is changed when sine waveform is intersects with high frequency triangular waveform

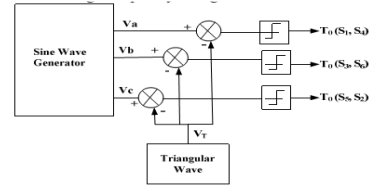


Fig.5 SPWM Control signal Generation

In 3-phase VSI, the SPWM is achieved by three sinusoidal voltages (Va, Vb, Vc) which are 120° out of phase with each other are compared with high frequency triangular waveform(VT), and relative levels of the waveforms are used to control the switching the devices in each phase leg of the inverter.

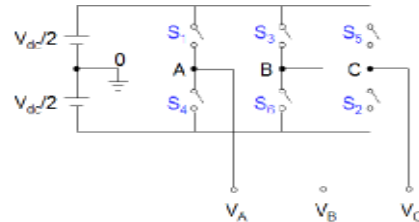


Fig.6 Three-phase Sinusoidal PWM inverter

Three phase VSI having six switches (S1-S6) with each phase output is connected to middle of the each inverter leg is shown in Fig.6. The output of the comparator forms the control signal for each leg of the inverter. In one leg, two switches makes a phase and these two switches open and close in a complementary fashion. The total voltage is Vdc, therefore the each pole voltage Vao, Vbo, Vco of the inverter varies between -Vdc/2and +Vdc/2. If the sine wave is greater than triangular wave, then upper switch is getting turned ON and lower switch is turned OFF. Based on switching states, positive or negative half DC link voltage is applied to each phase. Usually the switches are controlled in pairs (S1,S4),(S3,S6) and (S5,S2) and the logic is shown in Table I.

S1 is ON when Va>VT	when	S4 is OFF when Va<VT
S3 is ON when Va>VT	when	S6 is OFF when Va<VT
S5 is ON when Va>VT	when	S2 is OFF when Va<VT
S4 is ON when Va<VT	when	S1 is OFF when Va>VT
S6 is ON when	when	S3 is OFF when

$V_a < V_T$	$V_a > V_T$
S2 is ON when $V_a < V_T$	S5 is OFF when $V_a > V_T$

**Multilevel Inverters**

Multilevel converters have evolved as one of the promising industrial solutions for better dynamic performance and power quality demanding applications. A multilevel converter achieves high power ratings as well as enables the use of renewable energy sources. The basic principle of a multilevel converter to achieve higher power is to use a series of power electronic switches with several lower voltage dc sources to perform the power conversion by synthesizing a staircase voltage waveform. Capacitors, batteries, and renewable energy voltage sources can be used as the multiple dc voltage sources. A multilevel converter has several advantages over a conventional two-level converter. Multilevel converters can generate the output voltages with very low distortion, with reduction in dv/dt stresses across semiconductor devices. Multilevel converters produce smaller common mode voltage, and they draw input current with less harmonic distortion at a lower switching frequency.

**Flying capacitor MLI**

The classical flying capacitor multilevel inverter is shown in Fig.7. The number of switches are S1, S2, S3, S4, S1', S2', S3', S4'. Each leg has identical structure. And each series connected capacitors have a same voltage rating. And the three inner loop capacitors are C1, C2 and C3. And all the phases shared by equal dc link capacitors are C1, C2, C3 and C4 [15]. The voltage can be divided by  $V_{dc}/2$ ,  $V_{dc}/4$  and  $-V_{dc}/2$ ,  $-V_{dc}/4$  and  $V_{an}$ . The switches from S1- S4 are called upper arm main switches and switches from S1'- S4' are called lower arm auxiliary switches. [15]. And the voltages from classical MLI are five level output are based on the switching pattern and PWM signal. And the switches are conducts based on five different combinations.

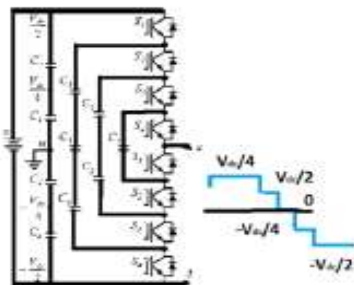


Fig.7 Classical Five level Flying Capacitor MLI.

And the voltage level  $V_{an}=0$ , it has six combinations, voltage level  $V_{an}= V_{dc}/2$ , it has one combinations and voltage level  $V_{an}= -V_{dc}/2$ , it has one combinations. Similarly for voltage level  $V_{an}=$

$V_{dc}/4$ , it has three combinations and voltage level  $V_{an}= -V_{dc}/4$ , it has three combinations respectively. Totally it consists of five output voltage levels. In this operation, during the positive and negative sign periods the capacitors can discharge and charge respectively.

**V. Matlab/Simulink Results**

*Case 1: Implementation of Proposed Concept using Neutral Clamped Type Multilevel Inverter.*

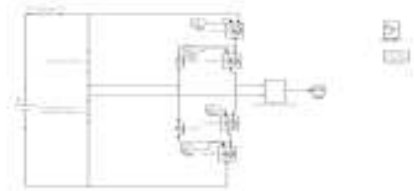


Fig: 14 Matlab/Simulink Model of Proposed 3level NPC Converter

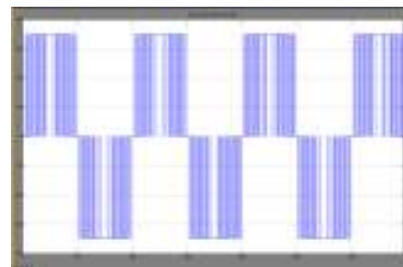


Fig:15 Output volge wave form of 3 level converter

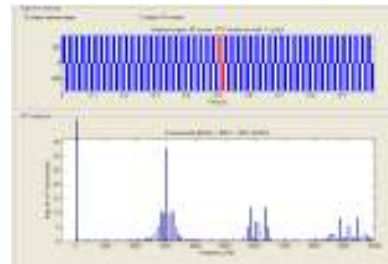


Fig. 16 FFT Analysis of Proposed 3 level NPC Converter Output Voltage

Fig. 16 shows the FFT Analysis of Proposed NPC Converter Output Voltage, we get 52.06% no need of any filter we get this value.

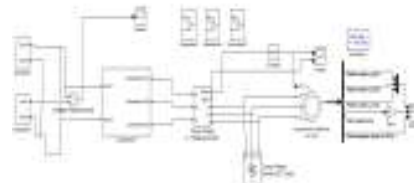


Fig. 17 Matlab/Simulink Model of Proposed 9-Level NPC Converter with Induction Machine Drive

Fig.17 shows the Matlab/Simulink Model of Proposed NPC Converter with Induction Machine Drive.

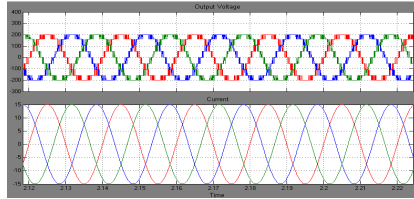


Fig.18 Level Output Voltage and Current

Fig. 18 shows the 9-Level Output Voltage and current coming from the proposed NPC multilevel inverter.

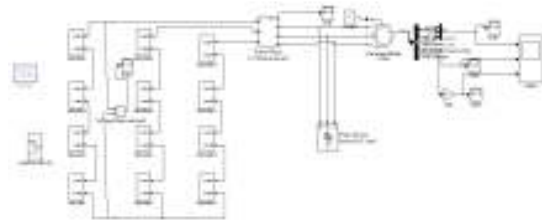


Fig: 24 Matlab/Simulink model of proposed 9-Level CHB converter with Induction Motor Drive

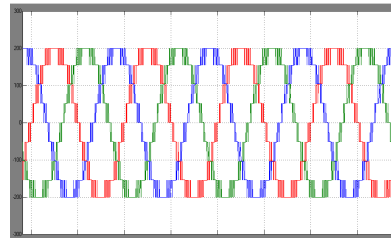


Fig. 25 Output Voltage of 9- Level CHB multilevel converter

Fig. 25 shows the 9-Level Output Voltage and coming from the proposed CHB Multilevel Inverter.

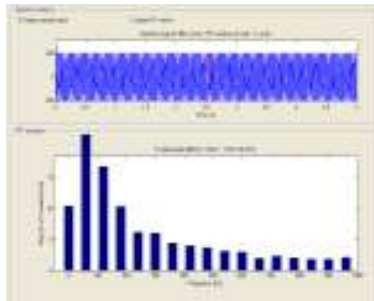


Fig. 20 FFT Analysis of Proposed NPC Converter Output Voltage

Fig. 20 shows the FFT Analysis of Proposed NPC Converter Output Voltage, we get 26.57% no need of any filter we get this value.

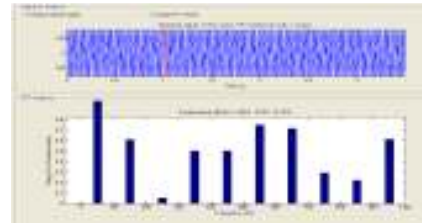


Fig. 26 FFT Analysis of Proposed CHB Multilevel Converter Output Voltage

Fig. 26 shows the FFT Analysis of Proposed CHB Multilevel Converter Output Voltage, we get 13.16% no need of any filter we get this value.

**Case 2: Implementation of Proposed Concept using Cascaded H-Bridge Multilevel Type Inverter**

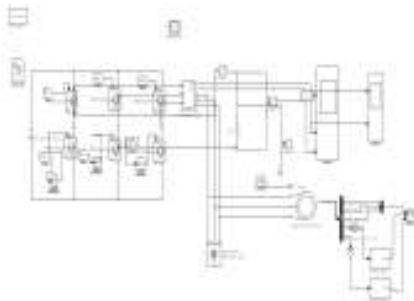


Fig: 21 Matlab/Simulink model of proposed CHB converter with Induction Motor Drive

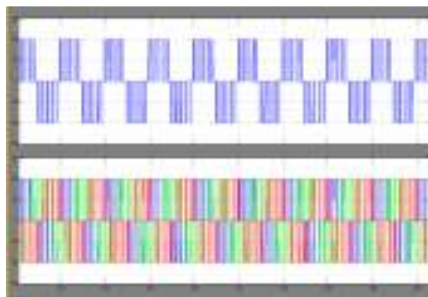


Fig. 22 shows the 3-Level Output Voltage from the proposed CHB multilevel inverter

**Conclusion**

Increasing demand on energy efficiency and power quality issues, grid connected solar PV systems is taking a good place. In this paper SPWM and SVPWM techniques have been discussed for 3-phase grid connected VSI. The LC filter circuit is used in the proposed system. This filter circuit is mathematically modeled by using state space analysis and complete state space equation is obtained. The SPWM technique is implemented and simulated on 3 phases VSI using state space model of the LC filter circuit for grid connected solar PV system. Various simulation results are analyzed and presented on the inverter and load side of the proposed system in order to demonstrate the satisfactory performance of sine-PWM technique for grid connected solar PV system.

**References**

[1] Ahmad, G. E., Hussein, H. M. S., El-Ghetany, H. H., Theoretical Analysis and Experimental

- Verification of PV Modules, *Renewable Energy*, 28(2003), 1159–1168.
- [2] Blaabjerg, F., Chen, Z., Kjaer, S., Power Electronics as Efficient Interface in Dispersed Power Generation Systems. *IEEE Trans. On Power Electronics*, 19(2004), no. 5, 1184-1194.
- [3] Hassaine, L., Olias, E., Quintero, J., Haddadi, M., Digital Power Factor Control and Reactive Power Regulation for Grid-Connected Photovoltaic Inverter, *Renewable Energy*, 34(2009), no. 1, 315-321.
- [4] Salas, V., Olias, E., Overview of State of Technique for PV Inverters Used in Low Voltage Grid-Connected PV Systems: Inverters Below 10kW, *Renewable and Sustainable Energy Rev.*, 13(2009), 1541-1550.
- [5] Gounden, N. A., Peter, S. A., Nallandula H., Krithiga, S., Fuzzy Logic Controller with MPPT using Line-Communicated Inverter for Three-Phase Grid-Connected Photovoltaic Systems, *Renewable Energy*, (2009), no. 34, 909-915.
- [6] Eltawil, M. A., Zhao, Z., Grid-connected Photovoltaic Power Systems: Technical and Potential problems-a review, *Renewable and Sustainable Energy Reviews*, 14(2010), no. 1, 112-129.
- [7] Sera, D., Tamas Kerekes, Marian Lungeanu, Pezhman Nakhost, Remus Teodorescu, Gert K. Anderson, Marco Liserre, Low-Cost Digital Implementation of Proportional-Resonant Current Controllers for PV Inverter Applications using Delta Operator, *IEEE Industrial Electronics Society Conference (IECON)*, (2005), 2517-2522.
- [8] Balouktsis, A., Karapantsios, T. D., Antoniadis, A., Balouktsis, I., Load Matching in a Direct-Coupled Photovoltaic System- Application to Thevenin's Equivalent Loads, *International Journal of Photoenergy*, (2006), 1-7.
- [9] El Amrani, A., Mahrane, A., Moussa, F. Y., Boukennou, Y., Solar Module Fabrication, *Int. Journal of Photoenergy*, (2007), 1-5.
- [10] Balouktsis, A., Karapantsios, T. D., Antoniadis, A., Paschaloudis, D., Bazergiannidou, A., Bilalis, N., Sizing Stand-Alone Photovoltaic Systems, *International Journal of Photoenergy*, (2006), 1-8.
- [11] K. Zhou and D. Wang, "Relationship Between Space-Vector Modulation and Three-Phase Carrier-Based PWM: A Comprehensive Analysis," *IEEE Transactions on Industrial Electronics*, Vol. 49, No. 1, pp. 186- 196, February 2002.
- [12] A.W. Leedy, and R.M. Nelms, "Harmonic Analysis of a Space Vector PWM Inverter using the Method of Multiple Pulses," *IEEE Transactions on Industrial Electronics*, Vol. 4, pp. 1182-1187, July 2006.
- [13] A.M. Khambadkone, and J. Holtz, "Current Control in Over-modulation Range for Space Vector Modulation based Vector Controlled Induction Motor Drives," *IEEE Industrial Electronics Society*, Vol.2, pp. 1134- 1339, 2000.
- [14] E. Hendawi, F. Khater, and A. Shaltout, "Analysis, Simulation and Implementation of Space Vector Pulse Width Modulation Inverter," *International Conference on Application of Electrical Engineering*, pp. 124-131, 2010.
- [15] B. P. McGrath and D. G. Holmes, "Analytical modeling of dynamics for a flying capacitor multilevel converter," *IEEE Trans. Power Electron.*, vol. 23, no. 2, pp. 543–550, Mar. 2008.